The Effect of Molybdenum Grain Characteristics on Ferroelectric $Al_{0.7}Sc_{0.3}N$ Film Properties

Minghua Li
*Institute of Microelectronics (IME), Agency for Science, Technology and Research (A*STAR), 2 Fusionopolis Way, Innovis #08-02, Singapore 138634, Republic of Singapore*
li_minghua@ime.a-star.edu.sg

Huamao Lin
*Institute of Microelectronics (IME), Agency for Science, Technology and Research (A*STAR), 2 Fusionopolis Way, Innovis #08-02, Singapore 138634, Republic of Singapore*
lin_huamao@ime.a-star.edu.sg

Binni Varghese
*Institute of Microelectronics (IME), Agency for Science, Technology and Research (A*STAR), 2 Fusionopolis Way, Innovis #08-02, Singapore 138634, Republic of Singapore*
Binni_Varghese@ime.a-star.edu.sg

Yao Zhu
*Institute of Microelectronics (IME), Agency for Science, Technology and Research (A*STAR), 2 Fusionopolis Way, Innovis #08-02, Singapore 138634, Republic of Singapore*
zhuya@ime.a-star.edu.sg

***Abstract*—Owing to the high coercive field of ferroelectric AlScN films, ultrathin (< 10 nm) is required for ferroelectric AlScN memory applications. High quality ultrathin film growth depends on the deposition parameters and the surface condition of the bottom electrode. In this work we fabricated $Al_{0.7}Sc_{0.3}N$ film on Mo electrode and found that the large and flat Mo (110) facet promoted heterogeneous nucleation of AlScN (0002) grains. On contrast, misaligned AlScN grains initialized in Mo grain boundary trench area. Our findings demonstrated the substrate impact on the AlScN film quality. Through bottom electrode texture and surface topography optimization, high quality ultrathin AlScN films can be obtained.**

Keywords—scandium aluminum nitride, ultrathin film, Mo bottom electrode, grain size, nucleation

I. Introduction

Scandium doped aluminum nitride (AlScN) has been demonstrated as an excellent ferroelectric material due to its high remnant polarization, large switching window, robust thermal stability, and CMOS compatible fabrication process. The coercive field ranges from 2 to 5 MV/cm, depending on the Sc doping concentration [1]. These values are relatively high compared to conventional ferroelectric materials. The coercive field values are about 0.05 and 1 - 2 MV/cm for lead zirconate titanate ($Pb(ZrTi)O_3$, PZT) and hafnium zirconium oxide ($Hf_{0.5}Zr_{0.5}O_2$, HZO), respectively [2]. Sub-10 nm thick AlScN films are required for practical ferroelectric device operation using on-chip driven voltage. Since the first report of ferroelectric AlScN with the thickness in hundreds nm [1], the ferroelectric switchable AlScN film thickness has been successfully reduced to sub-20 nm in 2020 [3], to 10 nm in 2021 [4], and further to 5 nm in 2023 [5]. About 1 V ferroelectric switching voltage has been achieved on ferroelectric capacitor structure containing 5 nm AlScN film [5]. All these achievements demonstrate that thickness downscaling is an effective approach to overcome the high coercive field challenge.

The coercive field and the remnant polarization show independence on the AlScN film thickness when the film is thick enough. However, when the AlScN film thickness decreases to ≤ 30 nm, higher coercive field and lower remnant polarization were measured [4 - 6]. Non-ferroelectric interfacial layer was suggested to be responsible for these changes [7].

Magnetron sputtering is the most commonly used technology for AlScN film deposition. The quality of film highly depends on the sputter conditions [8]. For sub-10 nm film deposition, heterogeneous nucleation process on different underlayer surface plays a critical role to improve the film quality and remove/reduce the non-ferroelectric interfacial layer. It has been reported [9] that improper plasma clean would damage the underlayer surface and generate 2-3 nm amorphous interface below the AlScN. This amorphous interface is surely non-ferroelectric switchable. Our previous investigation [10] has revealed that the initial 15-20 nm of the AlScN film deposited on bottom electrodes consists of smaller and tilt crystallites which may degrade the ferroelectric performance.

Thanks for the highly (0002) textured AlScN film grown on molybdenum (Mo) surface, good ferroelectric performance has been achieved in capacitor structure with Mo as bottom electrode [11]. In this work we sputter deposited $Al_{0.7}Sc_{0.3}N$ film on Mo surfaces and investigated the heterogeneous nucleation of AlScN (0002) crystallites. Optimization of Mo texture and surface topography were proposed to enhance the AlScN growth. Our findings would benefit high quality ultrathin AlScN film fabrication and high-performance device integration.

II. Experimental

A. AlScN film deposition on Mo electrode

AlScN and Mo films were deposited on 200 mm Si (100) wafers using a multi-chamber magnetron sputtering system. Prior to the 200 nm Mo film, a very thin layer of AlN was deposited as seed to promote Mo (110) texture. DC magnetron sputtering was used to deposit Mo film from a high purity Mo target. The surface roughness and Mo grain size can be adjusted by tuning the sputter condition.

After Mo deposition, the wafers were transferred without vacuum break into the AlScN chamber, where an $Al_{0.7}Sc_{0.3}$ alloy target was installed, and a pulsed DC power source was equipped. Both Ar and N_2 were introduced into the sputtering chamber as discharge and reactive gases for reactive sputter deposition of $Al_{0.7}Sc_{0.3}N$ films.

B. Characterization

X-ray Diffraction (XRD) and 4-point probe method were utilized to test the crystal structure and sheet resistance of the sputtered films, respectively. High-resolution Transmission Electron Microscopy (TEM) was used to investigate the AlScN/Mo interfaces. A dual beam Focused Ion Beam (FIB) machine was used to prepare samples for the TEM observation.

III. Results and Discussion

With the AlN seed layer, the sputtered Mo films showed good (110) texture regardless of the Mo grain size. Fig. 1 presents the XRD results of AlScN/Mo/AlN seed film stacks. Apart from the Si (004) peak from the substrate at 2θ = 69.1°, only Mo (110) (at 2θ = 40.7°) and AlN (0002) (at 2θ = 35.9°) reflection peaks were recorded, demonstrating well aligned out-of-plane Mo (110) and AlScN (0002) reflections. The rocking curve full-width-at-half-maximum (FWHM) of Mo (110) was about 1.7° for all samples.

Fig. 2 displays the sheet resistance measurement results. Large grain size facilitated lower sheet resistance of the Mo film, which can be attributed to the less grain boundary portion and the better crystalline structure [10].

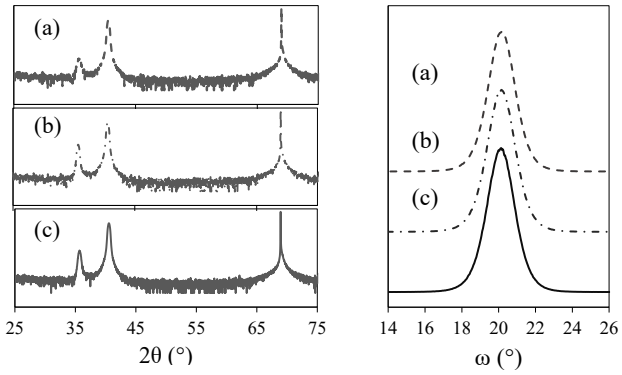

Fig. 1. XRD patterns (left) of Mo films with AlN seed layers and rocking curves of Mo (110) reflection peaks. From (a) to (c), Mo grain size increased without notable variation of the XRD patterns and rocking curve FWHM.

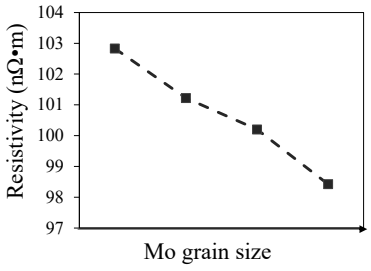

Fig. 2. Sheet resistance of 200 nm Mo films as a function of the Mo grain size. Lower resistivity was achieved on the film with larger grain and less grain boundaries.

Insightful investigation of Mo surface topography was performed using high resolution scanning TEM. Fig. 3 shows the cross-sectional images of 200 nm Mo films consisting of (a) small Mo grains and (b) large Mo grains. Flat (110) facet was found on the top surface of Mo grains. Trenches were found on top of the grain boundaries, as indicated by the yellow arrows. The density of the grain boundary trench depended on the Mo grain size. Small grain size led to high density of the grain boundary trench.

The high-resolution TEM image in Fig 4 (a) highlights the AlScN nucleation in a Mo grain boundary trench (Location 1) and on a flat Mo (110) facet (Location 2), respectively. At Location 1, tilt and misoriented AlScN crystallites were initialized from the Mo surface with crystallographic planes other than Mo (110). On contrast, (0002) textured AlScN tended to nucleate with the flat Mo (110) facet at Location 2. The corresponding fast-Fourier-transform diffraction (FFT) patterns as shown in Fig. 4 (b) and (c) further illustrated the difference in AlScN crystallinity at Location 1 and 2, respectively. Large Mo grains with flat (110) facet on the surface and less grain boundary trench promote the heterogeneous nucleation of (0002) AlScN grains.

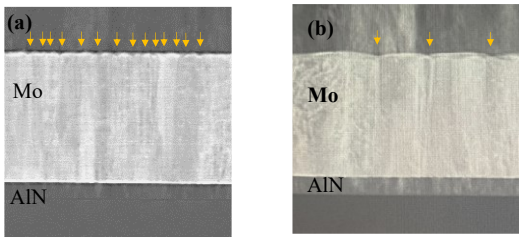

Fig. 3 Scanning TEM images showing 200 nm Mo films. The Mo grain size affects the surface topography.

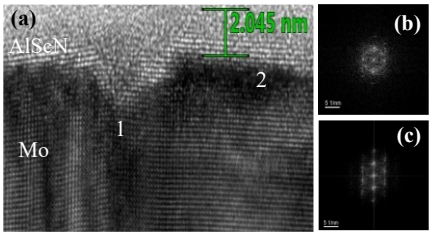

Fig. 4 (a) High-resolution cross-sectional TEM image of AlScN/Mo interface. Mo grain boundary trench and flat Mo (110) facet are showing at Location 1 Location 2 respectively. (b) and (c) the FFT patterns of initial AlScN crystallites grown in the Mo grain boundary trench and on the Mo (110) facet, respectively.

IV. Conclusions

Sputter deposition of $Al_{0.7}Sc_{0.3}N$ / Mo film stack was carried out. We found the crystal structure and the surface topography of Mo bottom electrode highly impact the AlScN nucleation and film (0002) texture. Large Mo grains provided more (110) facet area for AlScN (0002) nucleation, while the grain boundary trenches containing facets other than (110) led to misoriented AlScN crystallites. Our study provided valuable crystallographic information in the AlScN/Mo structure. Optimization of Mo grain facet condition could benefit ultrathin AlScN film growth and contribute to ferroelectric AlScN properties improvement.

ACKNOWLEDGMENT

This work was supported by the Science and Engineering Research Council of A*STAR (Agency for Science, Technology and Research), Singapore (Grant No. A20G9b0135).

REFERENCES

[1] S. Fichtner, N. Wolff, F. Lofink, L. Kienle, and B. Wagner, "AlScN: a III-V semiconductor based ferroelectric," J. Appl. Phys., vol. 125, pp. 114103, March 2019.

[2] T. Mikolajick, S. Slesazeck, H. Mulaosmanovic, M. H. Park, S. Fichtner, P. D. Lomenzo, M. Hoffmann, and U. Schroeder, "Next generation ferroeletric metarials for semiconductor process integration and their applications," J. Appl. Phys,, vol. 129, pp. 100901, March 2021.

[3] D. Wang, J. Zheng, P. Musavigharavi, W. Zhu, A. C. Foucher, S. E. Trolier-McKinstry, and R. H. Olsson III, "Ferroelectric switching in sub-20 nm aluminum scandium nitride thin films," IEEE Electron Device Lett., vol. 14, pp. 1774-1777, December 2020.

[4] R. Mizutani, S. Yasuoka, T. Shiraishi, T. Shimazu, M. Uehara, H. Yamada, M. Akiyama, O. Sakata, and H. Funakubo, "Thickness scaling of $(Al_{0.8}Sc_{0.2})N$ films with remanent polarization beyond 100 μCcm^{-2} around 10nm in thickness," Appl. Phys. Express, vol. 14, pp. 105501, September 2021.

[5] G. Schonweger, N. Wolff, M. R. Islam, M. Gremmel, A. Petraru, L. Kienle, H. Kohlstedt, and S. Fichtner, "In-grain ferroelectric switching in sun-5 nm thin $Al_{0.74}Sc_{0.26}N$ films at 1 V", arXiv:2304.02909 [cond-mat.mtrl-sci], April 2023.

[6] S. Yasuoka, T. Shimizu, A. Tateyama, M. Uehara, H. Yamada, M. Akiyama, Y. Hiranaga, Y. Chom and H. Funakubo, "Effects of deposition conditions on the ferroelectric properties of $Al_{1-x}Sc_xN$ thin films", J. Appl. Phys., vol. 128, pp. 114103, September 2020.

[7] M. Pirro, X. Zhao, B. Herrera, P. Simeoni, and M. Rinaldi, "Effect of substrate-RF on sub-200 nm $Al_{0.7}S_{0.3}N$ thin films," Micromachines, vol. 13, pp. 877, May 2022.

[8] S. K. Ryoo, K. D. Kim, H. W. Park, Y. B. Lee, S. H. Lee, I. S. Lee, S. Byun, D. Shim, J. H. Lee, H. Kim, Y. H. Jang, M. H. Park, and C. S. Hwang, "Investigation of optimum deposition conditions of radio frequency reactive magnetron sputtering of $Al_{0.7}Sc_{0.3}N$ film with thickness down to 20 nm," Adv. Electron. Mater., vol. 8, pp. 2200726, September 2022.

[9] K. Knisely, E. Douglas, J. Mudrick, M. Rodriguez, and P. Kotula, "Thickness dependence of $Al_{0.89}Sc_{0.12}N$ thin films grown in silicon", Thin Solid Films, vol. 675, pp. 66-72, February 2019.

[10] M. Li, H. Lin, J. Xie, W. Song, Y. Zhu, "Effects of post-annealing on texture evolution of sputtered ScAlN films," IEEE Int. Symp. Applications Ferroelectric (ISAF), July 2022.

[11] C. Liu, Q. Wang, W. Yang, T. Cao, L. Chen, M. Li, F. Lium D. K. Loke, J. Kang, and Y. Zhu, "Multiscale modeling of $Al_{0.7}Sc_{0.3}N$-based FeRAM: the steep switching, leakage and selector-free array", Proc. 2021 IEEE Int. Electron Devices Meeting (IEDM), USA, December 2021.